



Citation for published version:

Boiarkine, I, Norris, S & Patterson, D 2013, 'Investigation of the effect of flow structure on the photocatalytic degradation of methylene blue and dehydroabiatic acid in a spinning disc reactor', *Chemical Engineering Journal*, vol. 222, pp. 159-171. <https://doi.org/10.1016/j.cej.2013.02.025>

DOI:

[10.1016/j.cej.2013.02.025](https://doi.org/10.1016/j.cej.2013.02.025)

Publication date:

2013

Document Version

Peer reviewed version

[Link to publication](#)

NOTICE: this is the author's version of a work that was accepted for publication in *Chemical Engineering Journal*. Changes resulting from the publishing process, such as peer review, editing, corrections, structural formatting, and other quality control mechanisms may not be reflected in this document. Changes may have been made to this work since it was submitted for publication. A definitive version was subsequently published in *Chemical Engineering Journal*, 2013, vol 222, DOI 10.1016/j.cej.2013.02.025

University of Bath

General rights

Copyright and moral rights for the publications made accessible in the public portal are retained by the authors and/or other copyright owners and it is a condition of accessing publications that users recognise and abide by the legal requirements associated with these rights.

Take down policy

If you believe that this document breaches copyright please contact us providing details, and we will remove access to the work immediately and investigate your claim.

Investigation into the Effect of Flow Structure on the Photocatalytic Degradation of Methylene Blue and Dehydroabiatic Acid in a Spinning Disc Reactor

Irina Boiarkina^a, Stuart Norris^b, and Darrell Alec Patterson^c

^aDepartment of Chemical Engineering, University of Auckland, Engineering Building, 20 Symonds Street, Auckland, New Zealand, *iboi002@aucklanduni.ac.nz*

^bDepartment of Mechanical Engineering, University of Auckland, Engineering Building, 20 Symonds Street, Auckland, New Zealand, *s.norris@auckland.ac.nz*

^cCorresponding Author: Nanostructured and Tuneable Materials Laboratory, Department of Chemical Engineering and Centre for Sustainable Chemical Technologies, University of Bath, Claverton Down, Bath, BA2 7AY, United Kingdom, *D.Patterson@bath.ac.uk*

Abstract

The ultraviolet irradiated thin film coated spinning disc reactor is a new technology for the intensification of heterogeneous photocatalytic reactions. This reactor has previously been found to have a reaction rate maxima for the photocatalytic degradation of methylene blue across a spinning disc reactor. The reaction rate maxima occurred at an intermediate flow rate of 15mL/s and rotational speeds of 100 and 200rpm, where the reaction kinetics switched from first order to second order with a change in the flow structure. The findings of this work show that the reaction rate maxima is most likely in part caused by periodic forcing from the peristaltic pump increasing the mass transfer of the oxygen. The enhancement in the rate of oxygen transfer to the surface of the disc would increase the charge carrier separation in the catalyst, increasing the reaction rate kinetics. Oxygen being a second limiting reactant would also explain the presence of the second order kinetics. The flow regimes on the surface of the disc change between smooth, spiral and irregular waves depending on the flow rate and rotational speed. The effect of flow rate modulation only occurs when the flow is undisturbed by asymmetric outflow conditions interfering with the flow regime otherwise present on the disc. The initial surface rate of reaction for methylene blue was approximately $0.5 \times 10^{-7} \text{ mol/m}^2/\text{s}$ for most operational conditions, but the fast rate of reaction achieved with periodic forcing was $3.7 \times 10^{-7} \text{ mol/m}^2/\text{s}$, seven times greater than that achieved without the periodic forcing. Overall, this work shows that periodic forcing should be a key feature in achieving rate enhancements in spinning disc reactors, setting a new precedent in spinning disc reactor operational parameter choice.

Keywords: spinning disc reactor, dehydroabiatic acid, photocatalysis, process intensification, periodic forcing.

1 Introduction

Process intensification is a research area which has recently gained an increasing amount of interest. It focuses on improving efficiency and productivity, reducing the capital cost of process systems, improving intrinsic safety and minimising environmental impact [1, 2]. A review of different process intensification strategies can be found in [3].

Another area which continues to be researched for its potential for wastewater remediation is photocatalysis. Photocatalysis involves using light and a semiconductor catalyst to either partially degrade or fully mineralise waste in wastewater [4]. However the slow kinetics and difficulty in scale up have limited the application of this process [5, 6, 7]. The use of immobilised thin film catalysts has become increasingly popular to overcome the post separation step required with powders, however this leads to mass transfer limitations [6, 8, 7, 4, 9, 10].

A spinning disc reactor (SDR) is a process intensification technology where a liquid is fed to the centre of a horizontally rotating disc, causing it to spread out into a thin film. The film is highly sheared and this reactor shows enhanced heat and mass transfer characteristics [11, 12, 13], which makes the SDR of interest for mass transport limited reactions [11]. It is for these characteristics that the SDR was investigated for application as a thin film photocatalytic system [14] developing a novel photocatalytic SDR. Different flow regimes can form across the surface of the disc depending on the flow rate, rotational speed, and liquid properties [15, 14]. A previous publication [14] found that the photocatalytic surface rate of reaction in the photocatalytic SDR was independent of these flow regimes. However, a reaction rate maxima was found at the intermediate flow rate of 15mL/s, with investigated flow rates falling between 5 and 20mL/s. It was also found that aside from the fast first order reactions at 15mL/s, the overall kinetics were second order, which is unusual in photocatalysis. It was hypothesised that the reaction rate maxima was caused by a mass transfer effect, suggested by the reaction order switching, from second to first order for the reactions at these maxima.

Therefore, the main aim of this paper is to further investigate and characterise the photocatalytic SDR by investigating the source of the reaction rate maxima found in this previous work, as the high reaction rate at this flow rate dictates the desirable operational parameters. This could therefore indicate new optimal operating conditions and regimes that could be transferred across to optimise other SDR reaction systems.

The second aim of this work is to investigate source of the unusual second order kinetics and whether it was the result of the model compound, methylene blue. This was done by investigating the photocatalytic degradation of a different model compound, dehydroabietic acid (DHA), a resin acid found in pulp and paper wastewater. Resin acids are endocrine disruptors that have been shown to have adverse ecological effects at very low concentration [16, 17, 18]. The photocatalytic degradation of DHA has not been reported previously in the published literature. Consequently this work will also provide the benchmark photocatalytic degradation results for this important compound, which has wider relevance to the application of photocatalysis as a wastewater treatment technology in the pulp and paper industry.

All of the above further characterizes and expands the applications of this new photocatalytic process intensification technology and therefore comprises novel, innovative work in the area of photocatalysis, spinning disc reactors and process intensification.

2 Method and Materials

2.1 Materials

Methylene blue was obtained from Sigma-Aldrich (85% pure), DHA was obtained from Pfaltz and Bauer (USA), 90% pure and 99.5% pure oxygen by BOC gases was used for saturation of the reactant solution. The reagents used for TiO₂ sol preparation were glacial acetic acid (Univar, 99.7%), acetylacetone (Sigma-Aldrich, 99%), isopropanol (Univar, 99.7%), titanium isopropoxide (Aldrich, 97%) and deionised water (from an ELGA Maxima Ultra purifier system). The solvents used for analysis with high pressure liquid chromatography were trifluoroacetic acid (Sigma-Aldrich, 99%) and acetonitrile (Merck, 99.8%). All reagents were used as received.

2.2 Analytical Methods

The concentrations of methylene blue and DHA were quantified using a Shimadzu LC-20AT high pressure liquid chromatography unit (HPLC) with an SPL-20A UV-vis detector and the same Agilent Eclipse XDB-C18 column. For a detailed description of the analytical technique used for methylene blue detection, refer to [14].

The DHA method was based on the work of Shi [19], using an isocratic method composed of two mobile phases: a) Pure acetonitrile and; b) De-ionised water acidified with 0.01 vol% TFA. A total flow rate of 1mL/min composed of 80/20 mobile phases a/b was used with an injection rate of 100 μ L, an oven temperature of 25 °C and total analysis time of 15 minutes.

2.3 Experimental Set Up and Procedure

The sol-gel coating method described by Ling et al. [20] was used to immobilised the titanium dioxide catalyst on the surface of the glass discs to obtain a mechanically stable film. Heat treatment was carried out in a F.E. Kiln furnace with an RTC 1000 Bartlett Instruments Co. controller to obtain the photocatalytically active anatase crystal phase. SEM images of the deposited film showing the homogeneity of deposition can be found in [14].

A schematic of the experimental set up can be found in Figure 1. The experiments were run with complete recycle. The liquid was pumped from a 500mL stirred tank reservoir through a tightly sealed glass flask with a peristaltic pump. The glass flask acted as a buffer to dampen the flow pulsations. All transparent components of the system were wrapped with aluminium foil to prevent photolysis of the model compounds. The inlet pipe came in from the bottom of the reactor and went through the centre of the rotating shaft before coming out of the centre of the disc. This was to ensure no

shadowing of the UV light, which would have been unavoidable with the more traditional top feed tube. The inlet nozzle diverted the flow, so that the liquid hit the disc from above through an annular-shaped gap. The disc diameter was 200mm and the entire SDR was enclosed in an UV tight enclosure.

The reactor lid was fitted with a low pressure mercury UV lamp (20W, monochromatic, $\lambda=254\text{nm}$, Steriflow, supplied by Davey Water Products NZ, part nr. GPH369N/S) inside a quartz tube, with the lamp being situated at the focus of a parabolic mirror to improve the homogeneity of the irradiation. After reaction, the liquid was collected in a basin below the disc, and returned back to the reservoir by gravity. The reservoir was constantly sparged with oxygen to ensure that the solution was saturated. This was confirmed with a Mettler Toledo M0128 dissolved oxygen meter.

Prior to starting the reaction, the setup was run in the dark for 20 minutes for methylene blue or 30 minutes for DHA to allow for the adsorption of the model compound to reach equilibrium. The temperature of the reactant was kept at 27°C during the reaction with tap water using a Liebig cooler. For details on the equipment specifications, refer to [14].

The substrate concentrations used were 10mg/L ($26.74\mu\text{mol/L}$) of methylene blue. The DHA solution was prepared by dissolving 7mg of the as received DHA in 1L of water with 7mL of $2\text{w/v}\%$ NaOH, and stirring for 24 hours. The solution was then filtered through a #50 Whatman paper to remove any undissolved DHA.

2.4 Process and Kinetic Modelling

The reactor system had to be modelled in order to be able to compare the kinetic constants between runs, because of the variation of the flow rate and rotational speed. The modelling had to account for the dead time in the reservoir due to the very low residence time in the SDR, otherwise the reaction rate constants would have been artificially significantly lower than the real values.

The modelling approach followed that described in previous work [14], and the overall reaction rate constants extracted with this modelling encompassed the rate of light absorption, the oxidant and catalyst concentration and the mass transfer rate.

A mass balance can be performed on the system by treating the reactor and the reactant reservoir as separate control volumes. The reactant reservoir is assumed to behave as a perfectly mixed ideal continuously stirred tank (CST), with the outlet concentration equal to the bulk reservoir volume concentration. The change in concentration inside the reservoir with respect to time is given by,

$$\frac{dC_{INSDR}}{dt} = \frac{Q}{V_{CST}}(C_{OUTSDR} - C_{INSDR}), \quad (1)$$

where C_{INSDR} is the concentration inside the CST (and entering the SDR), C_{OUTSDR} is the concentration exiting the SDR (and hence entering the CST), Q is the volumetric flow rate and V_{CST} is the volume of the CST.

In order to model the SDR, the volume of liquid resident on the spinning disc had to be estimated. The Nusselt model (Equation 2) was used to predict the film height

across the spinning disc and assumes fully developed laminar flow across the surface of the disc with no shear at the gas-liquid interface [12].

$$h = \left(\frac{3Q\nu}{2\pi r^2 \omega^2} \right)^{\frac{1}{3}} \quad (2)$$

where h is the liquid film thickness, r is the radius across the disc, Q is the volumetric flow rate onto the disc, ν is the kinematic viscosity and ω is the rotational speed (rad/s).

Assuming that the SDR behaves as a plug flow reactor, a mass balance can be performed on a differential volume of the SDR in combination with Equation 2. This leads to the following expression for the change in substrate concentration with respect to radius across the SDR,

$$\frac{dC}{dr} = 2\pi \left(\frac{3\nu}{2\pi Q^2 \omega^2} \right)^{\frac{1}{3}} R''' r^{\frac{1}{3}}, \quad (3)$$

where R''' is the volumetric rate of reaction and the radius is r .

The kinetics were found to be second order, $R''' = k_v C^2$, which is uncommon in photocatalysis, for which first order reactions, reflecting a simplified Langmuir-Hinshelwood kinetic expression due to dilute reactant concentrations are the norm [6, 8]. Substituting second order kinetics into Equation 3 and integrating between the inlet and outlet radius, R_{IN} and R_{OUT} respectively, leads to the following expression for the reaction across the SDR:

$$C_{OUTSDR} = \frac{1}{2\pi k \left(\frac{3Q\nu}{2\pi \omega^2} \right)^{\frac{1}{3}} \left[R_{IN}^{4/3} - R_{OUT}^{4/3} \right] + \frac{1}{C_{INSDR}}} \quad (4)$$

Equation 4 was solved numerically in conjunction with Equation 1 to model the entire system with complete recycle. MATLAB code was used to fit k iteratively, and was improved from the code used in [14] as it solved only one equation numerically using ode45, an inbuilt ordinary differential equation solver based on the Runge-Kutta Dormand Prince method.

In heterogeneous catalysis with an immobilised catalyst, the kinetics can be expressed on a volumetric or surface area basis, where the surface area used is the illuminated surface area, not the surface area of the catalyst. This is done for comparison purposes as the use of surface reaction rate constants eliminates the effect of different reaction volume per surface area at different flow and rotational speed conditions on the spinning disc reactor. The reaction only occurs on the surface of the spinning disc. The surface rate constant can be calculated from the volume rate constant using Equation 5.

$$k_s = \frac{V}{S} k_v \quad (5)$$

where S is the illuminated surface area of the catalyst, k_s is the first or second order surface reaction rate constant, k_v is the first or second order volume reaction rate constant, and V is the volume of the reactor.

3 Results and Discussion

3.1 Degradation of Dehydroabiatic Acid in the Photocatalytic SDR

Experiments on the degradation of DHA were used to investigate the effect of the substrate on the degradation rate, specifically to clarify the source of the second order kinetics in previous work with the photocatalytic SDR with methylene blue, the high surface reaction rate maxima found, and characterise a wider range of the rotational speed (up to 350rpm) to quantify the effect on the rate of reaction.

Adsorption and photolytic control experiments can be found in Supplementary Material Figure A.1. Like the reactions of methylene blue in the photocatalytic SDR, kinetic fitting of the data showed that the DHA reactions followed second order kinetics, as shown in Figure 2, with first order kinetics showing a poor fit to the data (see supplementary material for further data). This means that the second order kinetics are not purely attributable to the model wastewater compound, and were not caused by the dimerisation of methylene blue, as was suggested as a possible mechanism in [14]. Indeed, this may indicate that the second order kinetics are a characteristic of the SDR. The hypothesised cause of the second order kinetics is discussed in further detail later, in Section 3.3. Before this can be done, a comparison between the characteristics of the photocatalytic reactions of methylene blue and DHA in the SDR and how this relates to the underlying hydrodynamics needs to be outlined in order to explain and isolate various factors that may contribute to the reaction kinetics.

Figure 3a shows the volume reaction rate constants plotted against the theoretical average film height across the surface of the disc. This graph shows that there is an increasing volume reaction rate with a decreasing liquid film height. The increasing volumetric rate of reaction is caused by a decreasing total volume, which is characterised by the average liquid film height. This is the same trend observed for methylene blue in this photocatalytic SDR [14]. The plotted error bars are one standard deviation from the average of repeat reactions carried out at the specified conditions. Figure 3a shows that the error increases with decreasing film height. This is likely caused by any small variations in the reaction rate being amplified by the increased recirculation for the same total reaction time, through the decreasing residence time (film height).

Surface area reaction rate constants, calculated using Equation 5, eliminate the effect of a varying reaction volume per surface area ratio at different reactor operational parameters. This makes a surface rate constant more representative of the performance of an immobilised heterogeneous catalyst. Figure 3b shows the effect of film height on the surface reaction rate constant of DHA.

Overall, Figure 3b shows that there is no visible correlation of the surface reaction rate of DHA with the film height. This is the same trend as found for the degradation of methylene blue [14]. This finding suggests that roughly the same number of pollutant molecules are degraded per pass of the SDR, giving a constant surface reaction rate.

There are two reactions that are fall outside of the range of error of the rest of the measurements: a) The lowest surface reaction rate constant was at the flow rate of 8mL/s and rotational speed of 100rpm and; b) The highest surface reaction rate constant was

at a flow rate of 20mL/s and rotational speed of 200rpm.

The reaction at a flow rate of 8mL/s corresponds to the highest residence time in the reactor and the lowest substrate recirculation rate. The lowest reaction rate at the flow rate of 8mL/s could be caused by a mass transfer limitation if the extra time spent in the reactor does not result in further degradation of the parent compound. In other words, the recirculation rate is too low for the overall rate of reaction.

No similar explanation can be given for the overall rate of reaction at a flow rate of 20mL/s and rotational speed of 200rpm. It has a residence time and a liquid film thickness that is intermediate between the other experiments. Figure 4a shows the effect of flow rate and rotational speed on the initial surface rate of reaction (5mg/L DHA). Figure 4c shows the average initial surface reaction rate plotted as a surface for the degradation of DHA, and complimentary contour plots may be found in Supplementary Material Figures B.1 and B.2. Although it would be expected that there would be an increasing surface rate of reaction at an increasing rotational speed and flow rate, due to increasing shear, such a trend is not visible on the graph. The data shows an approximately constant surface rate of reaction, with the majority of the experiments having an initial surface rate of reaction between 0.5 to 1×10^{-7} mol/ m²/s.

Figure 4d shows that the methylene blue reactions in the SDR also do not have an increasing rate constant with increasing rotational speed and flow rate, however, this is where the similarity ends. The two operating surfaces are very different, in particular, the DHA degradation not having the two reaction rate maxima at a flow rate of 15mL/s, as shown in Figure 4d. Thus the flow across the disc was investigated with a highspeed camera to determine if its structure had changed (either through changes as a result of using a different compound or perhaps changes in the SDR), which could have affected the rate of reaction.

Figures 4a and 4b can also be used to compare the degradability of DHA with that of methylene blue. The initial surface rates of reaction for DHA were calculated at 5mg/L and for methylene blue at 8mg/L. The molar initial concentrations between the two compounds are not significantly different, 16.7 μ mol/L and 21.4 μ mol/L for DHA and methylene blue respectively. As mentioned previously, the average initial surface rate of reaction for DHA is between 0.5 to 1×10^{-7} mol/ m²/s and Figure 4b shows that the average initial rate of reaction for methylene blue is also between 0.5 to 1×10^{-7} mol/ m²/s, when excluding the reaction rate maxima observed at 15mL/s. The degradation rates of the two compounds are comparable, even with the slightly higher concentration of methylene blue. This may be contributed to by the fact that the molecules are both three ringed structures with a similar molecular weight. Excluding the degradability of intermediates, it appears that the photocatalytic degradability of DHA in the photocatalytic SDR is similar to that of methylene blue.

3.2 Highspeed Camera Imaging: Change in Flow Across the Spinning Disc

A highspeed camera image study was carried out with the reactions carried out with the degradation of methylene blue reported in [14]. Similarly, a highspeed camera image study was also carried out with the degradation of DHA reported in this study. The

flow across the surface of the disc was found to be significantly different. Comparative photographs of flow in the SDR at the same operational parameters are shown in Figure 5.

Large standing waves can be seen in the photographs taken during the reactions with DHA in Figure 5. A close up schematic of the standing waves at a flow rate of 15mL/s and a rotational speed of 200rpm is shown in Figure 6. This is in contrast to the other types of waves observed (e.g. spiral, irregular and criss-cross) in the photographs taken during the methylene blue degradation experiments reported in [14], in which there is even flow outwards from the disc centre.

These standing waves are almost not visible at a combination of low flow rate and low rotational speed, as shown by Figure 5 at a flow rate of 5mL/s and rotational speeds of 50 to 150rpm. They are less severe at lower rotational speeds, for example at a flow rate of 20mL/s and rotational speeds from 50rpm to 150rpm shown in Figure 5. The standing waves were also obscured or disrupted by the other multitude of irregular waves at higher rotational speeds, such as at flow rates of 15 and 20mL/s and rotational speed of 350rpm, shown in Figure 5. The order of the severity of these waves on the disruption of the natural flow pattern by flow rate, from most severe, is 15mL/s, then 20mL/s and least severe at 5mL/s.

Close up images of the standing waves are shown in Figure 7, and show that the standing waves have a large smooth section behind the wave front. The standing waves were large, and could have flowed over and above the thin liquid film, hence introducing the smooth section found behind the wave front. This short circuiting of the flow may have interfered with the mass transfer normally present in the flow to the surface of the disc. The disruptive effect of the standing waves would be most pronounced at the flow rate of 15mL/s and mid range of rotational speeds (200rpm) as they are most severe in this region, which is where the most significant drop in reaction rate has taken place.

The standing waves originated from the nozzle, at a constant location with respect to the nozzle bolts. It was found that the main cause of the standing waves was due to the nozzle not being built to specification, with incorrect alignment between the top and bottom halves of the nozzle, as shown in Figure 8, resulting in an asymmetric annular outlet gap. The outflow asymmetry of the nozzle was also exaggerated by the differing release height relative to the disc surface, shown diagrammatically in Figure 8. The annular gap asymmetry was corrected with aluminium tape creating the more smooth ideal flow seen in the methylene blue results in [14]. However, the imperfect application of tape to adjust for this issue and gradual tape swelling, combined with the screws holding the nozzle pieces together gradually loosening up (from the constant screwing in and out during disc replacement) resulted in the change of flow across the surface of the disc and the aforementioned standing waves.

This change therefore created an opportunity to study how a different flow regime affected the reaction rates in the SDR, providing further information on how to control and optimise operating conditions in this new photocatalytic reactor system. Consequently, a new set of methylene blue reactions were conducted.

3.3 Effect of Change in Flow on the Degradation of Methylene Blue

Experiments were carried out to evaluate if the degradation rate of methylene blue had changed with the changed flow pattern across the surface of the spinning disc; to conclusively prove or disprove that the change in the rate of reaction trend at 15mL/s was caused by the change in model compound. The volume degradation rate constants of repeat methylene blue experiments at the same conditions as used in [14] are shown in Figures 9a and 9b.

The plotted volume reaction rate constants are averages of repeat reactions, however, not all reactions were repeated. For the repeat reactions, one standard deviation is provided as the error of the measurements for that respective data set. However, for non-repeated reactions, the error was taken as the *maximum* error of all available data.

It can be seen in Figure 9a that the majority of the two data sets do not overlap, as would be expected if the change in flow structure affected the reaction rate. Not all the changes are of equal weighting, or in the same direction, for different operational parameters. Thus, if the flow is changing the rate of reaction, it is not changing it uniformly across the different operational parameters. The three standing waves are almost not visible at the lower flow rates, as shown in Figure 7a. This could explain the reason why the reaction at a flow rate of 5mL/s and rotational speed of 200rpm (Figure 9a) shows the same performance despite the change in flow structure across the surface of the disc.

Figure 9b shows that the observed shifts in the reaction rates show no clear dependence on the average film thickness. The repeat reactions for methylene blue at a flow rate of 15mL/s show the same trend as the reactions found with DHA, that no reaction maxima occur here. This conclusively shows that the shape and type of flow must have had an effect on the overall rate of reaction. In order to confirm that the observed reactions effects were the result of the flow and nozzle outflow condition, the nozzle outflow was varied and the reactions at a flow rate of 15mL/s were repeated in order to systematically determine the flow characteristics that create the reaction rate maxima previously observed at these conditions.

3.4 Effect of Different SDR Nozzle Designs on Methylene Blue Degradation

The first modification was intended to increase the number of the standing waves present. This was done by throttling the flow through the outlet annular gap of the nozzle in a staggered formation, as shown in Figure 10a. The flow came out in series of jets onto the surface of the disc. This resulted in a doubling of the number of standing waves present. Figure 10b shows the effect that this had on the reaction rate at a flow rate of 15mL/s and rotational speed of 200rpm. The rate of reaction increased, outside of the expected error of repeat experiments, denoted by the error bars.

This improvement was not significant enough to improve the reaction rate to the level that was observed when the flow was mostly homogeneous in [14]. In order to overcome the inconsistent outlet height of the nozzle (as discussed in the previous section and shown in Figure 8), an aluminium cap was shaped and fitted over the top of the nozzle

to restrict the outlet flow at the surface of the disc to the same height in order to recreate the more homogeneous flow seen in the initial methylene blue experiments in [14]. A cross-sectional schematic diagram of the nozzle cap is shown in Figure 11. The nozzle cap was tested, without a reaction, to see if a stable flow could be maintained over the surface of the disc, without reverting to the presence of the standing waves observed during the DHA experiments so that when a reaction was carried out it could reliably be linked to a constant flow structure across the surface of the disc. Several reactions were then carried out with the aluminium cap at the same flow rate of 15mL/s and rotational speed of 200rpm, with differing flow structures across the surface of the spinning disc. The flow across the disc was noted during the reaction, and the results of these experiments are shown in Figure 12a, with diagrams of the observed flow structure shown in Figure 12b. Repeat reactions with the aluminium cap gave different flow structures due to the flexibility of the material. This therefore provided a greater range of flow structures to study. Some reactions such as reaction II in Figure 12 show fairly smooth flow with few waves, and other reactions such as V show a large number of small waves. From this, a trend was observed between more homogeneous flow (without the standing waves) and reaction rate: the general trend shown by Figure 12a is that the more homogeneous the flow appeared (and the fewer smaller waves present), and hence the closer to what it looked during the experiments reported in [14], the faster the reaction rate achieved. This makes sense, in part, less waves mean a surface that reflects and scatters less of the UV light, which should increase the UV penetration to the photocatalyst and therefore increase the reaction rate. This definitely shows that the outlet flow structure had a significant effect on the rate of reaction, as all other variables were kept constant. The effect of the nozzle on the flow structure is supported by literature: Lenewit et al. [21] found that wave formation was very sensitive to entrance conditions on a spinning disc reactor. This indicates that the nozzle design is a key parameter in the SDR and is consequently until now an overlooked characteristic that needs to be investigated in more detail in the future.

It should be noted that the reactions labelled V and VI were carried out with 700mL total system volume, and the rest with 550mL. Although this may introduce a confounding factor, this is unlikely because the modelling accounts for the change in system volume. It is also unlikely that the change in volume affects other kinetics parameters not accounted for by the modelling, or to a significant degree, because an equally low reaction rate is possible at a volume of 550mL, as shown by Reaction C with the nozzle cap (IV Figure 12b). Hence the conclusion remains the same, that a change in flow structure causes a change in the rate of reaction.

Therefore, the optimum flow for maximum reaction rate in this photocatalytic SDR is characterised by the first set of highspeed camera images reported in [14]: 1) The absence of large, standing pooled up waves; 2) A smooth region across the majority of the disc.

3.5 Determining if the Reaction is Mass Transfer Controlled

If the flow structure is improving the overall rate of reaction at 15mL/s, in addition to the increased light penetration described above, this is most likely due (in part at least) to mass transfer enhancement. This is because mass transfer resistances are a major factor that retard reaction rates in heterogeneous reactions systems [22, 4]. The standing waves, which are most severe at 15mL/s, probably interfere with this effect.

In order to test if the reaction is mass transfer controlled, and it is the enhancement in mass transfer rate that at least in part responsible for the change in reaction rate, the mass transfer rate can be compared with the overall reaction rate. The following assumptions are therefore made:

1. The reaction rate is first order with respect to the surface substrate concentration, which is true for the fastest reaction (although not for the rest).
2. The mass transfer rate of the substrate to the surface is proportional to the difference in concentration between the bulk solution and surface of the catalyst.
3. The mass transfer and the reaction steps happen in series.
4. The surface reaction is in equilibrium with the mass transfer.

Then the overall reaction rate constant is the inverse sum of the mass transfer rate and kinetic rate, shown by Equation 6. This is a common result, discussed in [22].

$$\frac{1}{k_{overall}} = \frac{1}{k_m} + \frac{1}{k_r} \quad (6)$$

This inverse summation ensures that the overall reaction coefficient will always be slower than *both* the mass transfer and kinetics rates. However, if the magnitude of one is significantly smaller than the other, then that rate will become limiting. Therefore, by comparing the overall rate to the mass transfer rate, the rate limiting factor can be determined.

The overall surface rate coefficient for the reaction at a flow rate of 15mL/s and rotational speed of 200rpm is 8×10^{-6} m/s. The mass transfer rates found experimentally by Burns and Jachuck for the flow across a spinning disc [23] were in the order of 0.16 to 0.35×10^{-3} m/s. Assuming that the mass transfer on this SDR model is of a similar magnitude, this indicates that the reaction *cannot* be limited by the mass transfer rate of the pollutant. The mass transfer rate of the pollutant is two orders of magnitude larger than the overall rate, hence the true reaction rate (i.e. the photocatalytic reaction rate at the surface of the TiO₂) must be limiting the overall rate of reaction. The enhancement in kinetics at 15mL/s with a change in flow is approximately seven times higher, as seen from Figure 12a, and it is not possible for the mass transfer of the pollutant to cause this improvement when it is not the limiting rate.

Therefore this indicates that the flow structure is changing the reaction rate on the surface of the catalyst. There are two likely explanations for this. Firstly, the change in UV penetration discussed above. Secondly, the photocatalytic reaction depends heavily

on the presence of an electron scavenger, normally oxygen [4]. It is normally assumed that the oxygen is not a limiting reactant, by using a saturated solution throughout the reaction. The solution was oversaturated with oxygen for the duration of these experiments, as measured with a dissolved oxygen meter. Oxygen, like methylene blue and DHA, needs to be mass transferred to the surface of the catalyst to perform its role as the electron scavenger. It separates the electron-hole pairs, decreasing electron-hole recombination and hence increasing the formation of active sites on the catalyst. Slow oxygen adsorption kinetics or slow electron transfer between the catalyst and adsorbed oxygen have often been found to be the rate limiting step in photocatalysis [24, 25, 26].

An improvement in the mass transfer rate of oxygen to the surface of the catalyst would directly impact the kinetics and reaction rate. An increase in mass transfer rate not only increases the mass transfer rate of the substrate, but also increase the mass transfer rate of the oxygen to the surface of the catalyst, and hence oxygen adsorption. An increase in the adsorption rate of oxygen would increase the reaction rate through an increase in the number of active sites present on the catalyst. The reaction between a pollutant molecule, A, and an active site * is shown in Equation 7.

$$-r = k[A][*] \quad (7)$$

The concentration of active sites available for the degradation of the parent compound [*] is inversely proportional to the concentration of active sites taken up by intermediates [I], which in turn is proportional to the degradation rate of the parent compound A: [*] \propto [I]⁻¹ \propto [A]. If the number of active sites available for the degradation of [A] decreases during the reaction, due to the formation of intermediates and low total site availability, then the degradation of [A] follows second order kinetics. However, if the formation of the active sites is faster than the total requirement of active sites for both the parent compound [A] and the intermediates, then the degradation rate of [A] will be independent of the total number of active sites and become first order. This would explain the presence of the second order kinetics observed for the reactions of both substrates, and also why the fastest reactions were first order. It is possible that the fastest reactions are first order because they are not limited by the formation of active sites due to slow oxygen adsorption. In this case the second order kinetics would be a kinetic disguise due to a physical process. Ollis has previously discussed how true chemical kinetics can be disguised by physical processes in [27]

3.6 Periodic Forcing Intensification

However, this still does not explain why there is an increase in the rate of reaction at 15mL/s in the initial methylene blue results. It is suggested that this is caused by periodic forcing, a known process intensification strategy discussed by Górak and Stankiewicz [3].

Górak and Stankiewicz's review [3] of process intensification discusses the introduction of dynamics, or artificial and purposeful periodicity, to improve reactor performance. They found that the inclusion of periodicity has been found to increase interfacial mass

transfer rates. Other authors have found that the introduction of specific frequency periodicity of system variables, such as pressure, temperature, flow rate and composition, can yield higher reactor performance [28, 29, 30, 31, 32, 33].

In this reactor strong periodic forcing could potentially be caused by the peristaltic pump, which created significant flow pulsation. Since it was assumed from the outset that a steady, non-pulsing flow was required (as is common in chemical reactor unit operations), a buffer was fitted in order to dampen these pulsations. However, this did not entirely eliminate them. As the enhanced rates both occurred at the same pump flowrate of 15mL/s, it is likely that there is a maxima in the pump pulsations through the buffer and into the system at this flow rate, enhancing the mass transfer rate through periodic forcing. This is also perhaps not the first time that periodic forcing has enhanced mass transfer rates in SDRs: Burns and Jachuck [23] also found elevated mass transfer rates at the lower flow rate of 10mL/s that they could not explain. This flow rate is close to the operating conditions in this work.

Literature on periodic forcing substantiates this hypothesis. A review by Silveston et al. [30] found that although periodic forcing on the flow rate is not an effective manipulated variable for single phase flow, it has been shown to be effective for two phase flows. Mathematical modelling carried out by Sisoiev et al. investigating the gas absorption into a wavy film flowing over a spinning disc found that waves deformed the boundary layer, improving the mass transfer rate [34]. In a different paper, the same authors studied (numerically) the effect of flow rate modulation and disc surface topography on the dynamics of the liquid film formed across the spinning disc [35]. They found that *intermediate* periodic forcing at the inlet gave an enhancement in the interfacial waviness, which was much higher than that found with constant flow rate. By inference, from the findings of Sisoiev et al. in [34], the larger interfacial waviness should result in enhanced mass transfer at intermediate periodic forcing conditions.

Burns and Jachuk [23], who found enhanced mass transfer at the lower flow rate, used a centrifugal pump with a needle valve for flow control. This means that the pump was constant speed, and thus the pulsations should be the same frequency across all flow rates. However, the pulsations may have a different magnitude due to the throttling of the flow by the needle valve, with the largest throttling at the lowest flow rate. Sisoiev et al. [34] also found that an increase in the amplitude of the periodic forcing (up to a finite limit) also increased the interfacial waviness, and by inference as per above the mass transfer. Therefore, in the work of Burns and Jachuk [23] it is more likely to be the amplitude, and not the frequency of the periodic forcing causing the mass transfer enhancement.

The enhanced rate of reaction found in the data in the current work corresponds to the intermediate flow rate conditions, where the peristaltic pump would have resulted in periodic forcing at an intermediate frequency. This may also explain why the presence of the standing waves destroys the enhanced rate of reaction; the standing waves may interfere with this effect by disrupting the periodically forced flow regime across the surface of the disc.

Further supporting evidence for this is also found in literature. Alekseenko et al. [36]

discusses the wave flow of liquid films on inclined planes, where much of the theory of thin film flow across a spinning disc originates from. Chapter 13 provides a discussion on the effect of waves on transfer processes, with experimental evidence of the effect of periodic perturbations on the mass transfer of dilute gases. The effect of waves on the mass transfer was disentangled from the effect of Reynolds number on the mass transfer, because any change in natural formation of waves is accompanied by a change in the flow conditions and hence Reynolds number as well. This was done by superimposing flow pulsations on the main flow, resulting in non-linear two-dimensional regular stationary waves covering the entire surface of the film. The characteristics of these waves were defined only by the frequency of the flow pulsations. They found that these ‘excited’ waves gave significant enhancements in mass transfer over the natural flow. The increase in the mass transfer depended on the period of the two-dimensional waves, with a larger wave period corresponding to a stronger intensification on the mass transfer, with long waves resulting in an increase of 150%. At high Reynolds number consistent intensification data could not be gathered due to the formation of three dimensional waves. The effect of three dimensional waves over two dimensional waves was studied experimentally by breaking down the two dimensional waves into three dimensional ones with the same period. It was found that the intensification was significantly larger for two dimensional waves. It is possible that for a spinning disc system the limit for three dimensional waves occurs at a flow rate of approximately 15mL/s. The flow rate of 15mL/s and rotational speeds of 100 and 200rpm are just at the transition from spiral to irregular regime, as shown in Figure 3 in [14]. As the flow rate and rotational speed are increased (beyond 200rpm) the nature of the waves becomes more three dimensional and irregular, weakening the enhancement of the periodic forcing as per the inclined plane case.

Another important parameter found by Alekseenko et al. [36] that affected the intensification was the path length of the film, with minimal intensification at the start, largest at the middle and then dropping off again to the end of the length. This means that the intensification does not occur over the entire area of the film. The larger the non-linearity of the waves, the larger the intensification of the mass transfer and the closer the maximum intensification occurs to the inlet. If this phenomena is translatable to the spinning disc system, then it is possible that at 15mL/s the mass transfer intensification is closest to the centre of the disc; which would mean that more of the disc surface experiences the enhanced rate of reaction compared with at other conditions. This is also substantiated by Leneweit et al. [21] who found that with higher flow rates or with strong inlet disturbances the wave development across the SDR takes on non-linear characteristics, in line with experiments performed on an inclined plane.

Therefore, it is possible that periodic forcing is causing an enhancement of the mass transfer of the oxygen, increasing the kinetics rate. The enhancement of the periodic forcing is most significant at the intermediate flow rate of 15mL/s, most likely because this forms the limit between where the waves are most non-linear to where the waves become three dimensional, which sets a preferred condition for the operational flow rate of the reactor to get maximum mass transfer rate enhancement.

4 Conclusions

Two model compounds were investigated for the photocatalytic degradation in a SDR, methylene blue and DHA. It was found that both compounds showed a similar degradation rate, mostly likely due to a similar three-ringed molecular structure and similar molecular weight. The degradation of both model compounds were used to evaluate the source of the reaction rate maxima found at the intermediate flow rate of 15mL/s and it was found that the flow structure affects the rate of reaction across the surface of the disc. It is hypothesised that the reaction rate maxima is the result of periodic forcing from the peristaltic pump enhancing the mass transfer of the oxygen combined with conditions characterised by a more homogeneous flow regime. The more homogeneous flow regime would also decrease light scattering and hence increase penetration of the UV light to the catalyst surface. The enhanced oxygen would improve the charge carrier separation and through that the reaction rate kinetics, resulting in the enhanced rate of reaction. The effect of flow rate modulation only occurs when the flow is undisturbed by asymmetric outflow conditions short circuiting the flow. This makes the nozzle design an important design consideration in SDRs, which is normally overlooked. The initial surface rate of reaction for methylene blue is approximately $0.5 \times 10^{-7} \text{ mol/m}^2/\text{s}$ for most operational conditions, but the fast rate of reaction achieved with periodic forcing is $3.7 \times 10^{-7} \text{ mol/m}^2/\text{s}$, which seven times larger than that achieved without the periodic forcing. Periodic forcing should be investigated as a possible method of intensifying reaction kinetics, for the spinning disc reactor and other reactors, as its enhancement effect is on top of the increased mass transfer already normally observed in this system.

5 Acknowledgements

The authors would like to acknowledge the University of Auckland Doctoral Scholarship supporting Irina. The authors would also like to acknowledge Allan Clendinning, Ray Hoffmann, Peter Buchanan, Laura Liang and Frank Quin for technical help, the University of Auckland's Faculty of Engineering Workshop for fabricating the reactor and Jessie Mathew and Cecilia Lourdes for administrative help at the Department of Chemical Engineering.

References

- [1] C. Brechtelsbauer, N. Lewis, P. Oxley, F. Ricard, and C. Ramshaw, "Evaluation of a spinning disc reactor for continuous processing," *Organic Process Research & Development*, vol. 5, no. 1, pp. 65–68, 2000.
- [2] A. Aoune and C. Ramshaw, "Process intensification: heat and mass transfer characteristics of liquid films on rotating discs," *International Journal of Heat and Mass Transfer*, vol. 42, no. 14, pp. 2543–2556, 1999.

- [3] A. Górak and A. Stankiewicz, “Intensified reaction and separation systems,” *Annual Review of Chemical and Biomolecular Engineering*, vol. 2, pp. 431–451, 2011.
- [4] A. Mills and S. Le Hunte, “An overview of semiconductor photocatalysis,” *Journal of Photochemistry and Photobiology A: Chemistry*, vol. 108, no. 1, pp. 1–35, 1997.
- [5] T. Van Gerven, G. Mul, J. Moulijn, and A. Stankiewicz, “A review of intensification of photocatalytic processes,” *Chemical Engineering and Processing*, vol. 46, no. 9, pp. 781–789, 2007.
- [6] A. Ali, E. A. C. Emanuelsson, and D. A. Patterson, “Photocatalysis with nanostructured zinc oxide thin films: The relationship between morphology and photocatalytic activity under oxygen limited and oxygen rich conditions and evidence for a Mars van Krevelen mechanism,” *Applied Catalysis B: Environmental*, vol. 97, no. 1-2, 2010.
- [7] C. McFarlane, E. A. C. Emanuelsson, A. Ali, W. Gao, and D. A. Patterson, “Understanding the rate, mechanism and reuseability of zinc oxide nanostructured films as photocatalysts for industrial wastewater treatment,” *International Journal of Chemical Engineering*, vol. 2, pp. 63–79, 2010.
- [8] A. M. Ali, E. A. C. Emanuelsson, and D. A. Patterson, “Conventional versus lattice photocatalysed reactions: Implications of the lattice oxygen participation in the liquid phase photocatalytic oxidation with nanostructured ZnO thin films on reaction products and mechanism at both 254nm and 340nm.,” *Applied Catalysis B: Environmental*, vol. 106, no. 3-4, pp. 323–336, 2011.
- [9] D. D. Dionysiou, G. Balasubramanian, M. T. Suidan, A. P. Khodadoust, I. Baudin, and J.-M. Lainé, “Rotating disk photocatalytic reactor: development, characterization, and evaluation for the destruction of organic pollutants in water,” *Water Research*, vol. 34, no. 11, pp. 2927–2940, 2000.
- [10] D. D. Dionysiou, A. A. Burbano, M. T. Suidan, I. Baudin, and J. M. Lainé, “Effect of oxygen in a thin-film rotating disk photocatalytic reactor,” *Environmental Science & Technology*, vol. 36, no. 17, pp. 3834–3843, 2002.
- [11] K. V. K. Boodhoo and R. J. Jachuck, “Process intensification: spinning disk reactor for styrene polymerisation,” *Applied Thermal Engineering*, vol. 20, no. 12, pp. 1127–1146, 2000.
- [12] J. R. Burns, C. Ramshaw, and R. J. Jachuck, “Measurement of liquid film thickness and the determination of spin-up radius on a rotating disc using an electrical resistance technique,” *Chemical Engineering Science*, vol. 58, no. 11, pp. 2245–2253, 2003.
- [13] I. Tsibranska, D. Peshev, G. Peev, and A. Nikolova, “Modelling of mass transfer in film flow of shear thinning liquid on a horizontal rotating disk,” *Chemical Engineering and Processing: Process Intensification*, vol. 48, no. 3, pp. 823–827, 2009.

- [14] I. Boiarkina, S. Pedron, and D. A. Patterson, "An experimental and modelling investigation of the effect of the flow regime on the photocatalytic degradation of methylene blue on a thin film coated ultraviolet irradiated spinning disc reactor," *Applied Catalysis B: Environmental*, vol. 110, pp. 14 – 24, 2011.
- [15] A. Charwat, R. Kelly, and C. Gazley, "The flow and stability of thin liquid films on a rotating disk," *Journal of Fluid Mechanics*, vol. 53, no. 2, pp. 227–255, 1972.
- [16] A. Kostamo and J. Kukkonen, "Removal of resin acids and sterols from pulp and mill effluents by activated sludge treatment," *Water Research*, vol. 37, pp. 2813–2820, 2003.
- [17] M. Ali and T. R. Sreekrishnan, "Aquatic toxicity from pulp and paper mill effluents: a review," *Advances in Environmental Research*, vol. 5, no. 2, pp. 175–196, 2001.
- [18] A. Werker and E. R. Hall, "Limitations for biological removal of resin acids from pulp mill effluent," *Water Science and Technology*, vol. 40, no. 11-12, pp. 281–288, 1999.
- [19] H. Shi, "The photocatalytic degradation of dehydroabiatic acid in an annular reactor: comparing between three titanium dioxide photocatalyst configurations," Master's thesis, University of Auckland, 2011.
- [20] C. M. Ling, A. R. Mohamed, and S. Bhatia, "Performance of photocatalytic reactors using immobilized TiO₂ film for the degradation of phenol and methylene blue dye present in water stream," *Chemosphere*, vol. 57, no. 7, pp. 547–554, 2004.
- [21] G. Leneweit, K. G. Roesner, and K. R., "Surface instabilities of thin liquid film flow on a rotating disk," *Experiments in Fluids*, vol. 26, pp. 75–85, 1999.
- [22] O. Levenspiel, *Chemical Reaction Engineering*. Wiley, New York, 3rd ed., 1999.
- [23] J. R. Burns and R. J. J. Jachuck, "Determination of liquid-solid mass transfer coefficients for a spinning disc reactor using a limiting current technique," *International Journal of Heat and Mass Transfer*, vol. 48, no. 12, pp. 2540–2547, 2005.
- [24] A. Mills, J. Wang, and D. F. Ollis, "Dependence of the kinetics of liquid-phase photocatalysed reactions on oxygen concentration and light intensity," *Journal of Catalysis*, vol. 243, pp. 1–6, 2006.
- [25] D. F. Ollis, "Photocatalytic purification and remediation of contaminated air and water," *Surface Chemistry and Catalytics*, vol. 3, pp. 405–411, 2000.
- [26] D. Monllor-Satoca, R. Gomez, M. Gonzalez-Hidalgo, and P. Salvador, "The "direct-indirect" model: An alternative kinetic approach in heterogeneous photocatalysis based on the degree of interaction of dissolved pollutant species with the semiconductor surface," *Catalysis Today*, vol. 129, pp. 247–255, 2007.

- [27] D. F. Ollis, “Kinetic disguises in heterogeneous photocatalysis,” *Topics in Catalysis*, vol. 35, pp. 217–223, 2005.
- [28] J. E. Bailey, F. J. M. Horn, and R. C. Lin, “Cyclic operation of reaction systems: Effects of heat and mass transfer resistance,” *American Institution of Chemical Engineering Journal*, vol. 17, pp. 818–825, 1971.
- [29] J. E. Bailey and F. J. M. Horn, “Improvement of the performance of a fixed-bed catalytic reactor by relaxed steady state operation,” *American Institution of Chemical Engineering Journal*, vol. 3, pp. 550–553, 1971.
- [30] P. Silveston, R. R. Hudgins, and A. Renken, “Periodic operation of catalytic reactors - introduction and overview,” *Catalysis Today*, vol. 25, pp. 91–112, 1995.
- [31] P. Kocí, M. Kubíček, and M. Marek, “Periodic forcing of three-way catalyst with diffusion in the washcoat,” *Catalysis Today*, vol. 98, no. 3, pp. 345–355, 2004.
- [32] P. L. Silveston and R. R. Hudgins, “Periodic pressure forcing of catalytic reactions,” *Chemical Engineering Science*, vol. 59, pp. 4055–4064, 2004.
- [33] V. P. Zhdanov, “Periodic perturbation of the kinetics of heterogeneous catalytic reactions,” *Surface Science Reports*, vol. 55, pp. 1–48, 2004.
- [34] G. M. Sisoiev, O. K. Matar, and C. J. Lawrence, “Gas absorption into a wavy film flowing over a spinning disc,” *Chemical Engineering Science*, vol. 60, no. 7, pp. 2051–2060, 2005.
- [35] O. K. Matar, G. M. Sisoiev, and C. J. Lawrence, “Thin film flow over spinning discs: The effect of surface topography and flow rate modulation,” *Chemical Engineering Science*, vol. 63, no. 8, pp. 2225–2232, 2008.
- [36] S. V. Alekseenko, V. E. Nakoryakov, and B. G. Pokusaev, *Wave Flow of Liquid Films*. Begell House, New York, 1994.

List of Figures

1	Schematic diagram of the experimental set up.	20
2	Comparison example between first and second order reaction kinetics fitted to the degradation of DHA at a flow rate of 15mL/s and rotational speed of 350rpm in the spinning disc reactor.	21
3	Effect of film thickness on the volume and surface reaction rate constants a) volume rate constants b) surface area rate constants.	22
4	Effect of flow rate and rotational speed on the surface rate constants of the degradation of methylene blue and DHA a) DHA b) methylene blue from [14] c) DHA average initial reaction rate surface plot d) methylene blue from [14] average initial reaction rate surface plot.	23
5	Comparative photographs of flow regimes during the degradation of methylene blue in [14] and during the degradation of DHA.	24
6	A schematic of the standing waves at a flow rate of 15mL/s and rotational speed of 200rpm, with an outline of one of the standing waves and arrows designating the other two.	25
7	Close-up comparative photographs of flow regimes during the degradation of methylene blue in [14] and during the degradation of DHA assuming UV light does not affect the surface tension/flow characteristics a) 5mL/s and 200rpm with methylene blue b) 5mL/s and 200rpm with DHA c) 15mL/s and 100rpm with methylene blue d) 15mL/s and 100rpm with DHA e) 20mL/s and 350rpm with methylene blue f) 20mL/s and 350rpm with DHA.	26
8	Schematic diagram of the side and top views of the inlet nozzle showing the asymmetric annular gap and differing liquid release height - h	27
9	Initial surface reaction rates of repeated reactions with methylene blue after the change in flow regime a) effect of flow rate and rotational speed b) effect of estimated film thickness.	28
10	Effect of staggered nozzle outflow obstructions on the degradation rate of methylene blue at 15mL/s and 200rpm a) showing staggered nozzle obstruction arrangement b) effect of arrangement on rate of reaction.	29
11	Cross-sectional schematic of the nozzle cap fitted over the top of the nozzle, to restrict the outflow to the same height.	30
12	Diagrams showing a) The effect of flow structure on the surface rate of reaction of methylene blue at 4mg/L (half initial starting concentration) b) The flow structure observed during those reactions.	31

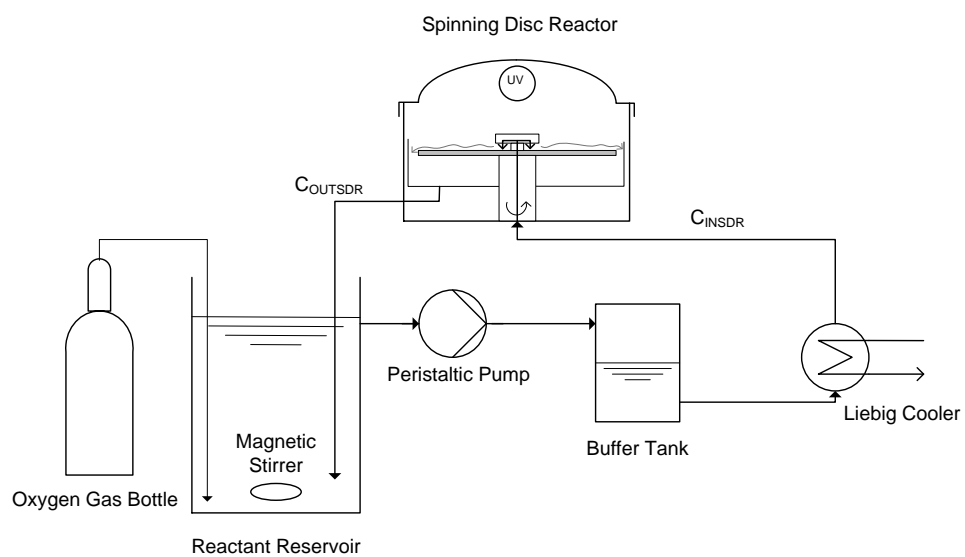


Figure 1: Schematic diagram of the experimental set up.

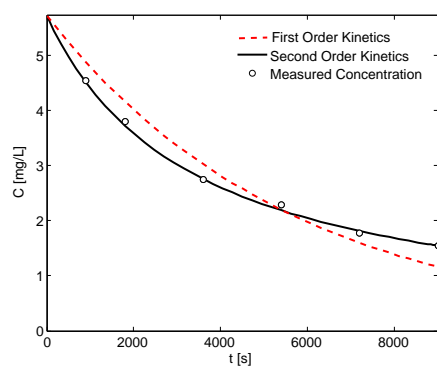
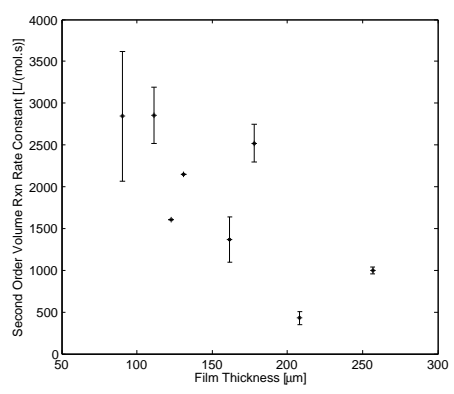
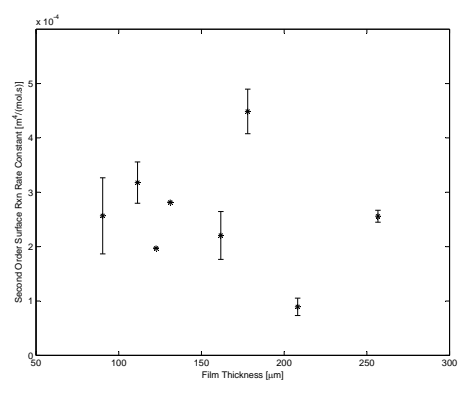


Figure 2: Comparison example between first and second order reaction kinetics fitted to the degradation of DHA at a flow rate of 15mL/s and rotational speed of 350rpm in the spinning disc reactor.

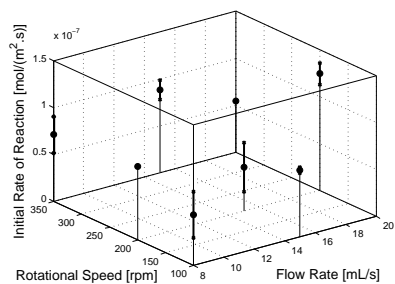


(a)

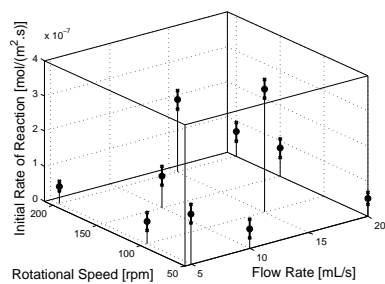


(b)

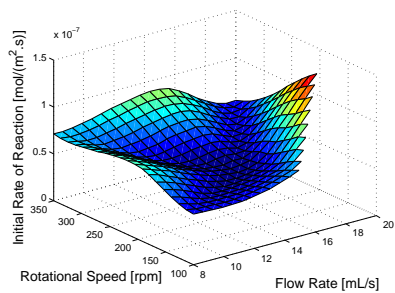
Figure 3: Effect of film thickness on the volume and surface reaction rate constants a) volume rate constants b) surface area rate constants.



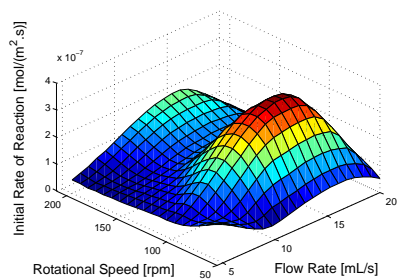
(a)



(b)



(c)



(d)

Figure 4: Effect of flow rate and rotational speed on the surface rate constants of the degradation of methylene blue and DHA a) DHA b) methylene blue from [14] c) DHA average initial reaction rate surface plot d) methylene blue from [14] average initial reaction rate surface plot.




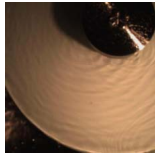
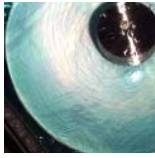
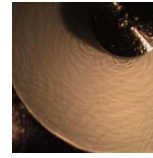

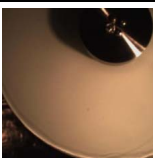



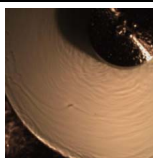

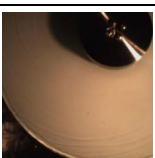

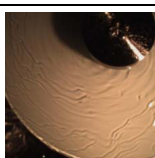

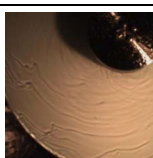
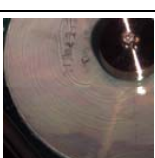
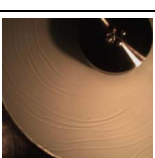
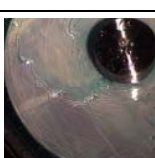
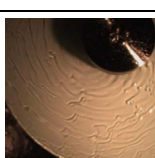
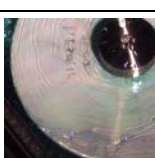
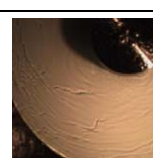
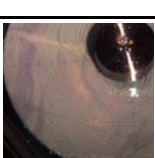

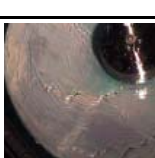
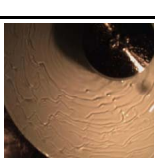


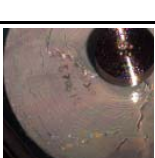
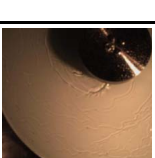

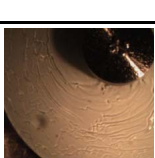
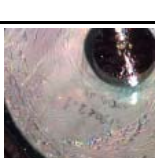
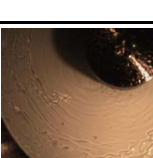
Flow Rate	5 mL/s		15mL/s		20mL/s	
Rot Speed	DHA Experiments	Methylene Blue Experiments	DHA Experiments	Methylene Blue Experiments	DHA Experiments	Methylene Blue Experiments
50rpm						
100rpm						
150rpm						
200rpm						
250rpm						
350rpm						

Figure 5: Comparative photographs of flow regimes during the degradation of methylene blue in [14] and during the degradation of DHA.

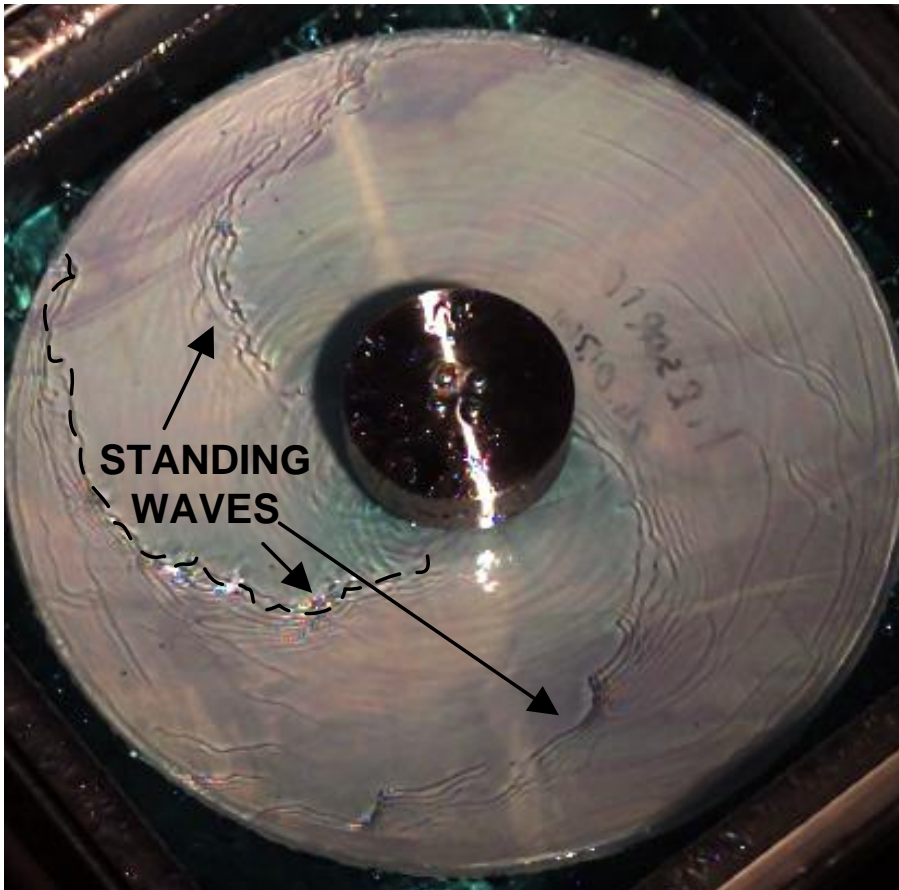


Figure 6: A schematic of the standing waves at a flow rate of 15mL/s and rotational speed of 200rpm, with an outline of one of the standing waves and arrows designating the other two.

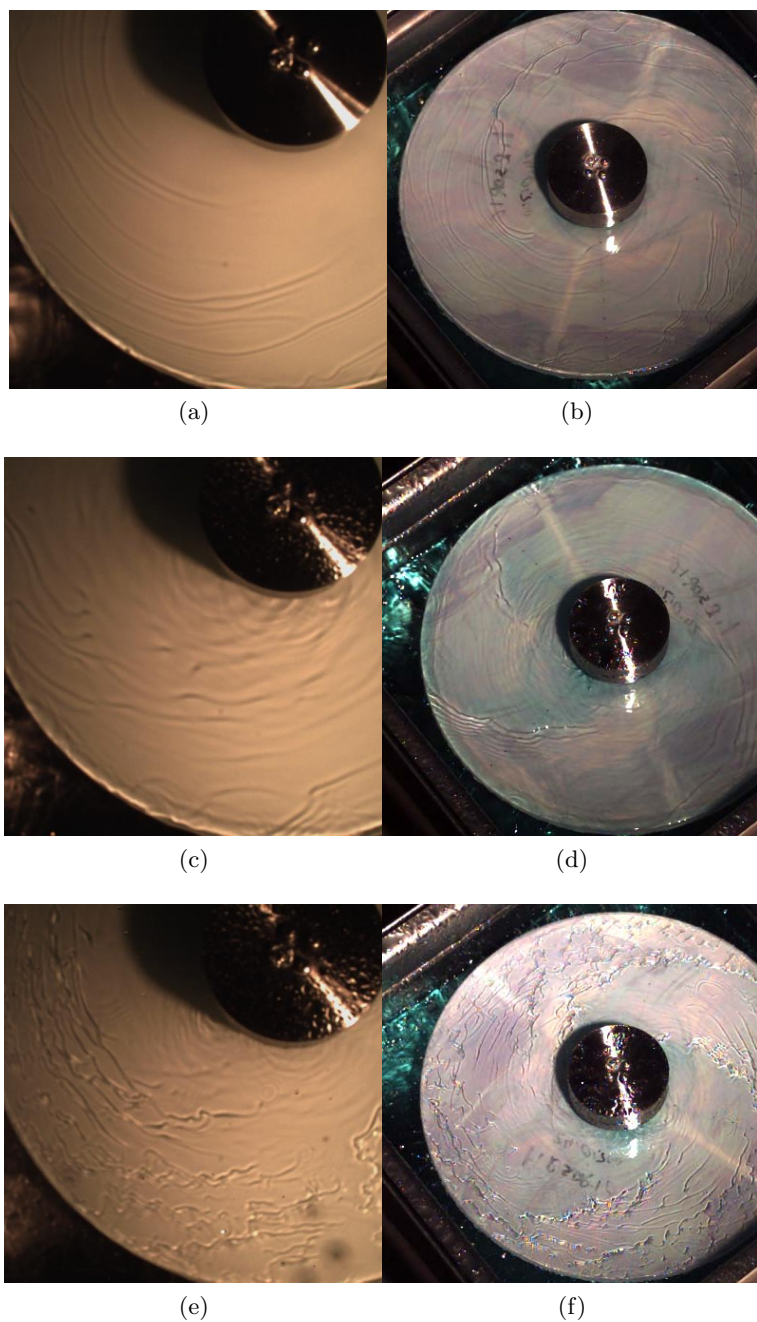


Figure 7: Close-up comparative photographs of flow regimes during the degradation of methylene blue in [14] and during the degradation of DHA assuming UV light does not affect the surface tension/flow characteristics a) 5mL/s and 200rpm with methylene blue b) 5mL/s and 200rpm with DHA c) 15mL/s and 100rpm with methylene blue d) 15mL/s and 100rpm with DHA e) 20mL/s and 350rpm with methylene blue f) 20mL/s and 350rpm with DHA.

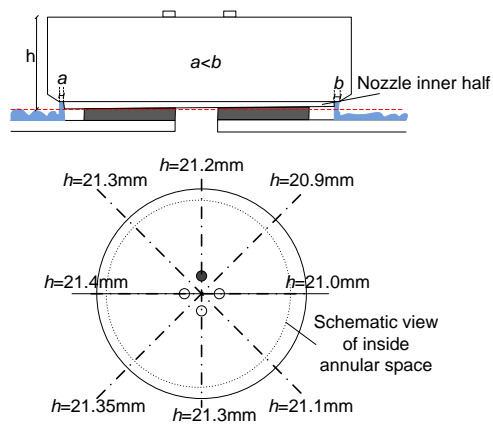


Figure 8: Schematic diagram of the side and top views of the inlet nozzle showing the asymmetric annular gap and differing liquid release height - h .

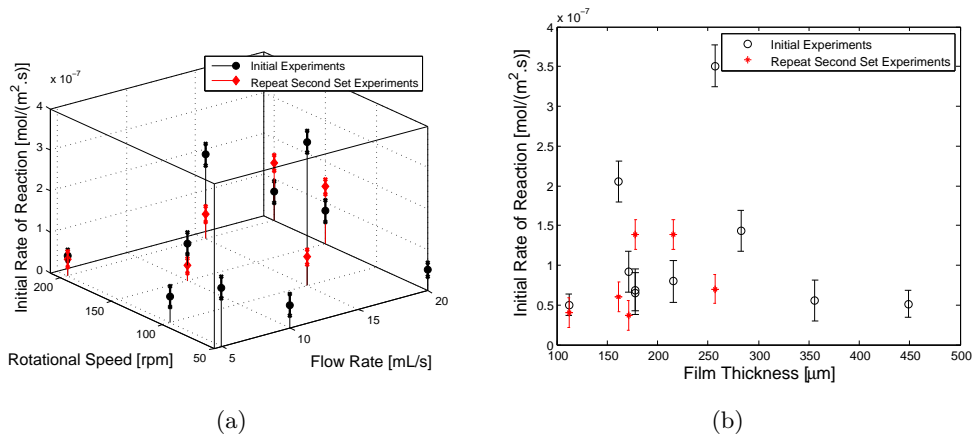


Figure 9: Initial surface reaction rates of repeated reactions with methylene blue after the change in flow regime a) effect of flow rate and rotational speed b) effect of estimated film thickness.

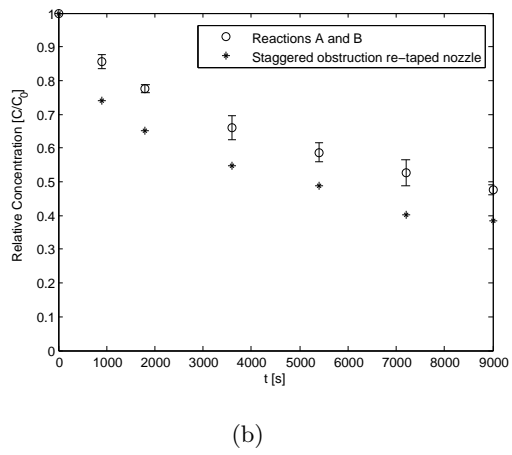
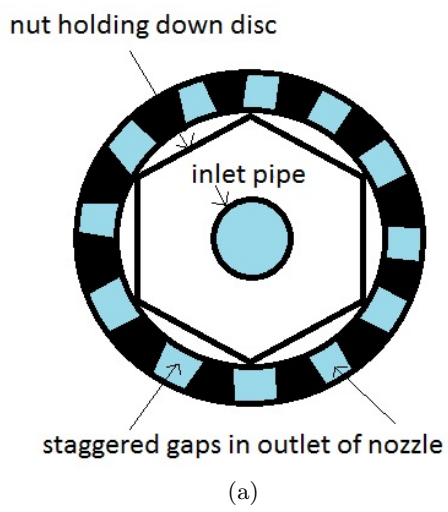


Figure 10: Effect of staggered nozzle outflow obstructions on the degradation rate of methylene blue at 15mL/s and 200rpm a) showing staggered nozzle obstruction arrangement b) effect of arrangement on rate of reaction.

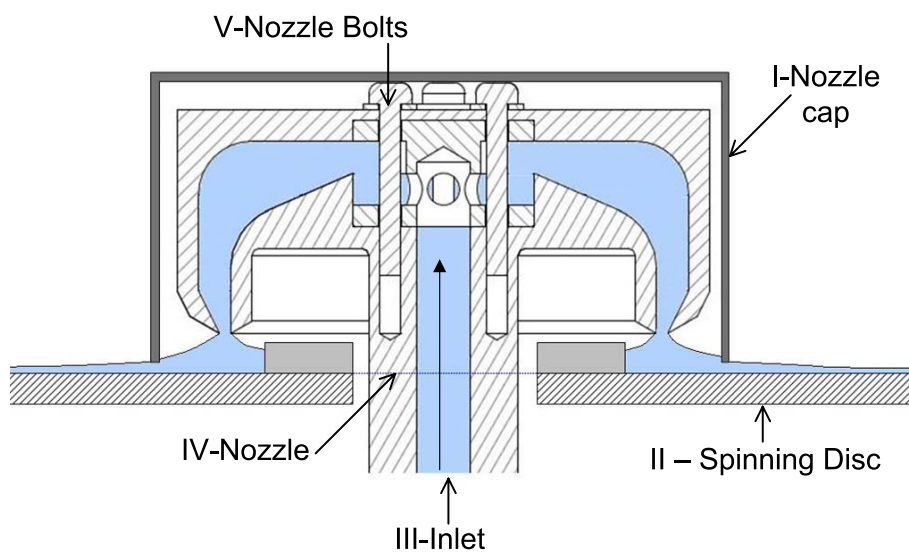
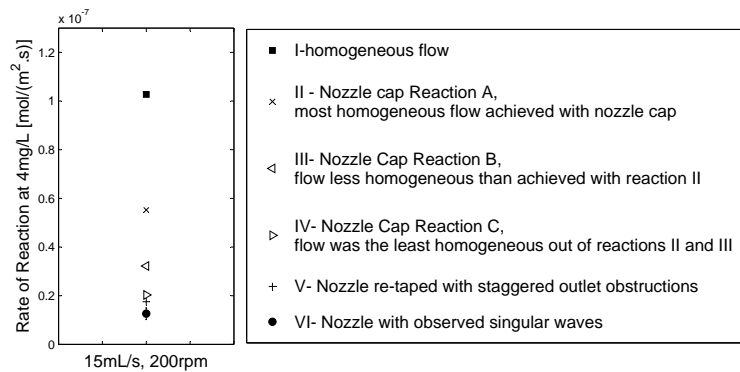
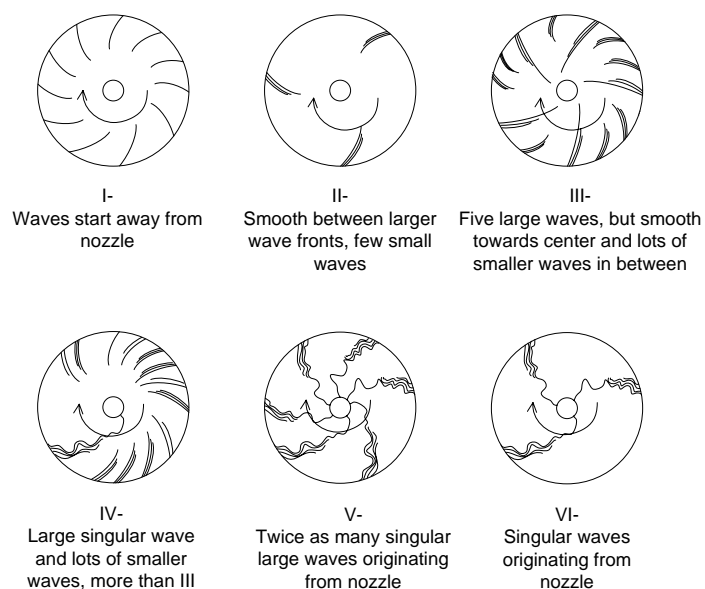


Figure 11: Cross-sectional schematic of the nozzle cap fitted over the top of the nozzle, to restrict the outflow to the same height.



(a)



(b)

Figure 12: Diagrams showing a) The effect of flow structure on the surface rate of reaction of methylene blue at 4mg/L (half initial starting concentration) b) The flow structure observed during those reactions.